INTEGRATING HIGH-RESOLUTION TASKABLE IMAGERY INTO A SENSORWEB FOR AUTOMATIC SPACE-BASED MONITORING OF FLOODING IN THAILAND

Steve Chien [(1)], David Mclaren[(1)], Joshua Doubleday[(1)], Daniel Tran [(1)], Veerachai Tanpipat[(2)], Royol Chitradon[(2)], Surajate Boonya-aroonnet[(2)], Porranee Thanapakpawin[(2)], Daniel Mandl[(3)]

[(1)] Jet Propulsion Laboratory, California Institute of Technology,
4800 Oak Grove Drive, Pasadena, CA, 91109-8099, USA, Email: {firstname.lastname}@jpl.nasa.gov
[(2)] Hydro Agro Informatics Institute, Bangkok, Thailand, Email: {veerachai,royol,surajate,porranee}@haii.or.th
[(3)] Goddard Space Flight Center, 8800 Greenbelt Road, Greenbelt, MD, 20771, USA, Email:Daniel.mandl@nasa.gov

ABSTRACT

Several space-based assets (Terra, Aqua, Earth Observing One) have been integrated into a sensorweb to monitor flooding in Thailand. In this approach, the Moderate Imaging Spectrometer (MODIS) data from Terra and Aqua is used to perform broad-scale monitoring to track flooding at the regional level (250m / pixel) and EO-1 is autonomously tasked in response to alerts to acquire higher resolution (30m/pixel) Advanced Land Imager (ALI) data. This data is then automatically processed to derive products such as surface water extent and volumetric water estimates. These products are then automatically pushed to organizations in Thailand for use in damage estimation, relief efforts, and damage mitigation.

More recently, this sensorweb structure has been used to request imagery, access imagery, and process high-resolution (several m to 30m), targetable asset imagery from commercial assets including Worldview-2, Ikonos, Radarsat-2, Landsat-7, and Geo-Eye-1. We describe the overall sensorweb framework as well as new workflows and products made possible via these extensions.

1. INTRODUCTION

Flooding has a tremendous impact on humanity and is worldwide in scale. Thailand (as well as greater southeast Asia) is particularly prone to flooding as observed during the 2010 and 2011 flooding seasons in Thailand. The Thailand flooding of October-November 2010 [1-3] was responsible for over 200 deaths, over $1.67 Billion USD damage, and affected over 7 million people [4]. The Thailand flooding in 2011 was even more severe (See Figure 1) accounting for over 600 deaths and $45.7 Billion USD damage [5] as of February 2012 the full damage is likely to be considerably higher.

This paper describes the paradigm of *sensorweb operations* in which sensing, interpretation, modeling, and tasking, are automated in a closed loop fashion to enable improved environmental modeling. We describe these key steps of automation as well as ongoing efforts to integrate additional satellite sensors, in-situ sensors, and hydrological modeling to tracking and modeling of flooding for both humanitarian and scientific purposes.

2. SPACE-BASED MONITORING OF FLOODING

A number of satellites have been used to track flooding at a global or regional scale: most notably QuikSCAT (Quick Scatterometer), The Advanced Microwave Scanning Radiometer for Earth Observing System (AMSR-E), and Moderate Resolution Imaging Spectrometer (MODIS). This work includes [6-12] Additionally AMSR-E [13] and The Tropical Rainfall Measurement Mission (TRMM) enable measurement of rainfall and therefore can be used as indicators of flooding.

Radars such as Radarsat-2, Environnmental Satellite (ENVISAT)/Advanced Synthetic Aperture

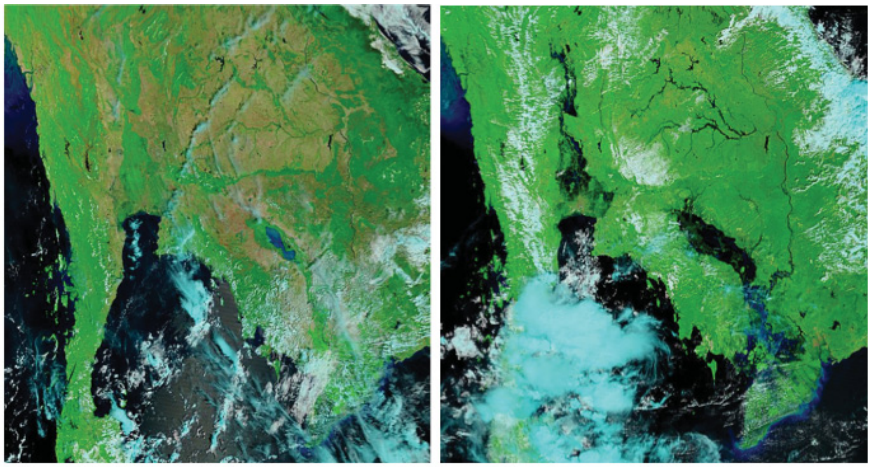

Dry: March 6, 2011 Flooded: October 27, 2011

Figure 1: Flooding in Southeast Asia, Fall 2011

Radar (ASAR) and Advanced Land Observation Satellite (ALOS) / Phased Array type L-band Synthetic Aperture Radar (PALSAR) have both been used to detect surface water extent from flooding. Radar has the advantage of being able to gather accurate data even in the presence of cloud cover.

Landsat-5, Landsat-7, and Earth Observing One (EO-1)/Advanced Land Imager (ALI) can all be used to detect surface water using spectral methods. While these sensors provide higher resolution data (30m/pixel) their infrequent revisit rate and challenge with clouds limit their utility for global flood mapping.

In-situ sensors can also provide valuable information. In-situ sensors can provide point estimates of rainfall, water levels, and in some cases flow rates.

Hydrological modeling is an essential part of flood management. Hydrological models are typically grid-based water balance models that track incoming water from rainfall or from upslope, water lossage from evaporation or absorption, and outflow (downslope). Hydrological models are critical in that they enable tracking the movement of the water downstream and thus can provide warning as flood waters move from highlands to lower lying plains, a frequent occurrence in Thailand. All of the sources of data we have described in this section (e.g. satellite, in-situ) can be considered inputs to the hydrological models.

3. SENSORWEB – THE CONCEPT

In our sensorweb concept (see Figure 2), the sensorweb constantly assimilates available data from any and all available sources to track flooding. This may be as easy as downloading the available data. Or it may mean active querying to determine if potentially contributing satellites are acquiring data and acquiring the data from relevant servers when available. Data acquisition may also involve downloading in situ data from the web. This data is used to constantly update our model of the flood state. All of these data can then be combined with hydrological models to perform hindcasting (estimation of flood parameters in the past to fill in missing times or areas), nowcasting (estimating the current flood state by using the model to fill in spatial gaps), and forecasting (using the model to predict which areas are at risk for future flooding).

When appropriate, the raw data and model are used to generate specific flood products for end users such as local, regional, and national authorities. These products may include surface water extent maps, flood alerts for already inundated areas, and alerts for areas at future risk. When targetable satellite assets are potentially available, the sensorweb can automatically request data.

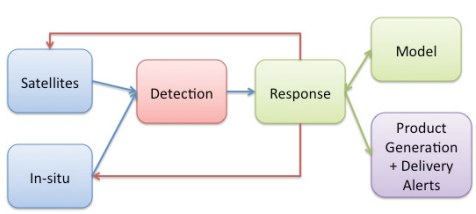

Figure 2: Sensorweb Paradigm

Key elements of the sensorweb concept are:

1. Automated detection of events or features of interest
2. Automated reconfiguration of the network (tasking) based on the automated detection (1.).
3. Automated Product generation and delivery

The key benefits of the sensorweb concept are:

1. the sensorweb by partially and fully automated means enables automatic acquisition of higher spatial resolution, swath-limited data in response to flooding. This higher resolution data can be used for a range of flood response purposes including damage estimation, mitigation, and allocation of response resources.
2. The sensorweb automatically processes a wide range of data and provides it to the authorized users in the format and with the analysis they need. Instead of getting a large number uncorrelated raw imagery sources, the users have surface water extent, water depth, depth analysis geo-referenced data. Resultant shape filed can be ingested into their GIS systems and they also have access to a tool that enables them to query the estimated water depth of any point.

3.1 The Thailand Flood Sensorweb – A Pilot Operational Sensorweb

We have operated a sensorweb to monitor flooding in Thailand for the 2010 and 2011 [14] flooding seasons (roughly beginning in May and ending as late as spring the following year). The core of this system uses the MODIS and EO-1/ALI sensors and leverages the unique automated tasking capability of EO-1. Other sensors including Worldview-2, Geo-Eye-1, Ikonos, Landsat-7, and Radarsat-2 have been integrated in a less automated fashion. These sensors and assets are combined with automated workflows to deliver satellite imagery, surface water extent products, and surface water volume products to relevant entities in Thailand. The success of this core system has led to ongoing work to add additional sensors and data products such as TRMM, river basin and sub-basin hydrological models, and data from in-situ sensor networks. Below we describe the core operational sensorweb and ongoing efforts to expand the sensorweb.

3.2 Automated Flood Detection Using MODIS

Our primary sensorweb flood alert mechanism is triggering via analysis of MODIS imagery. MODIS s provides excellent temporal coverage (at least 2x per day daylight overflights). We draw the subsetted FAS Indochina MODIS data in geotiff format from the MODIS rapid response site (originally rapidfire and now LANCE-MODIS). This imagery is then analyzed and surface water pixels compared to baseline dry season levels to detect flooding [14]. Figure 1 shows the band 7-2-1, surface water extent maps derived from MODIS data for dry and flooded imagery.

3.3 Automated Tasking of the EO-1 Satellite

The Earth Observing One spacecraft is the core of our sensorweb because of its automated tasking capability [15-16]. EO-1 is automatically tasked from each MODIS flood detection. The Thailand flood sensorweb MODIS alerts comprise a sensorweb campaign [15] within the EO-1 tasking system and therefore each alert can cause an observation request with an assigned mission priority. In order to operationally prioritize Thailand Flood Sensorweb requests, we divided the target sites into several major zones and the highest priority alerts from each zone are forwarded to the EO-1 sensorweb tasking system. Because EO-1 is a point and shoot spacecraft with limited agility, it is unlikely to be able to observe multiple geographically close targets (because of slow maximum slew rates). Therefore the pre-filtering of Thailand flood targets by geographic zone prevents Thailand flood scenes from competing amongst themselves. EO-1 was tasked requesting pointing centering the Advanced Land Imager (ALI) Instrument (30km wide swath, 30m spatial resolution multispectral, 9 bands 0.4-2.4 μ m spectral range) on the target site of the alert.

Each tasking request for EO-1 is considered in the context of other competing tasking requests and spacecraft operations constraints [16] – including pointing, maneuver, data storage, thermal, and timing. The automated tasking system can accept requests 24/7 and continuously attempts to maximize acquisition of high priority images. Note that EO-1 also has an onboard flood detection system capability using the Hyperion sensor [17] that is not used for the flood sensorweb primarily due to the limited Hyperion image swath width.

Our flood detection and tracking system was also used manually and semi-manually to request observations from other satellite assets (most notably Worldview-2). However, EO-1's automated tasking capability (and tasking availability and authority) enabled its key role in the sensorweb.

3.4 Automated Estimation of Surface Water Extent in Worldview-2, Ikonos, Geo-Eye-1 Imagery

We applied Support Vector Machine Learning (SVM) [18] techniques to learn classifiers to automatically detect flooded areas in Earth Observer One (EO-1) Advanced Land Imager (ALI) data [14] and Worldview-2 data [19].

Scenes of ALI and Worldview-2 data from regions of Thailand were collected and hand labeled for water (large lakes or catchments), developed areas, undeveloped ground, cloud, and finally cloud shadowed regions. In the interest of producing products that may be useful in flood mitigation, labels for ground and water were chosen aggressively through partially clouded observations. Labeling, training, validation (quantitative and qualitative) and kernel-parameter selection, was done through the Pixellearn tool [20].

Several datasets (Worldview-2, Ikonos, Geo-Eye-1) have been analyzed using band ratio surface water extent classification techniques. In this approach the ratio of the green to near infra-red spectral bands is thresholded to discriminate between land and water. Figure 3 (upper left, lower left, lower right) show automatically derived surface water extent maps from Worldview-2 imagery. Both the SVM and band ratio methods show good accuracy. Figure 4 (left, middle) show Geo-Eye-1 imagery and band ratio derived surface water extent product. Figure 5 (left, middle) shows Ikonos imagery and derived surface water extent product.

Satellite/Sensor	Green Band (nm)	Near IR Band
EO-1/Hyperion	550	860
EO-1/ALI	525 - 605	845 - 890
Worldview-2	510 -580	770-895
Ikonos	506 - 595	757 – 853
Geo-Eye-1	510 - 580	780 - 920
Landsat-7 ETM+	525 - 605	750 - 900

3.5 Automated Derivation of Water Volume from Surface Water Extent and Digital Elevation Information

We have created a workflow that uses surface water extent classification results from a sensor (including MODIS, ALI, WV2, or Radarsat2 raster GeoTIFFs), calculates pixel heights using a digital elevation model (DEM), and estimates the depth of flood-water pixels by estimating their elevation from their boundary. Because the program reads classified images as input, it generalizes well to a large suite of instruments: any classification data that can be saved in a GeoTIFF can be used in this approach. We tested this system using scenes of flooding in Bangkok during October-November 2011. We obtained a DEM of the Bangkok & Ayutthaya region of Thailand, with 5m horizontal and 1m vertical resolution, from Thailand's

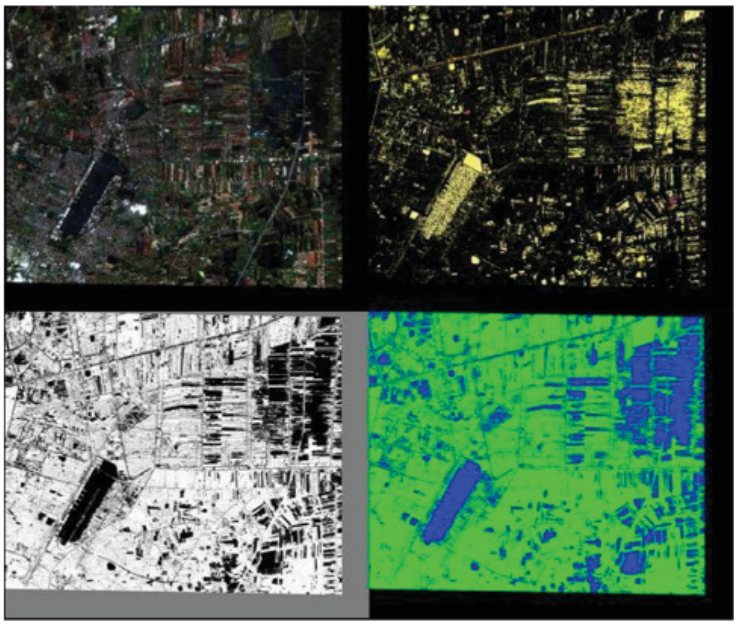

Figure 3: RGB image of WV-2 scene (Catalog ID: 2020010090403A00) taken November 3, 2011 (upper left);
water depth map: pale yellow = 0 meters, blue = 9m (upper right);
band ratio water extent map: black=water (lower left),
SVM surface water extent map: green=land, blue=water (lower right)

Hydro and Agro Informatics Institute (HAII).

For the Thailand sensorweb, we automatically receive ALI data acquired by the EO-1 satellite along with the SVM derived surface water extent (as described above). Unfortunately, the ALI images are poorly registered, often requiring manual registration of the images by fixing them against shapefiles of road and permanent water body data using ArcGIS.

We semi-automatically acquire and process data from a range of other sources including Radarsat-2, ALOS-PALSAR, Worldview-2, Ikonos, and Geo-Eye-1. For these datasets

The procedure used to estimate water depths of flooded pixels is roughly as follows (see [19] for further details):

1. Identify all land, water, and no-data pixels from classification results.
2. Identify all (land or water) pixels at a land-water boundary.
3. Identify all connected bodies of water within the image.
4. For all water and boundary pixels (*i,j*), estimate the height of the pixel *h[i,j]*, using the following procedure. Given a geolocated DEM and the input classification image's horizontal resolution *R* (in meters), we estimate height by finding the nearest pixel in the DEM corresponding to the lat-lon location of *(i,j)* in the classification map, constructing a box around this pixel with side length *R*, and setting *h[i,j]* to the average of all the DEM pixel values found inside this region.
5. For each water body f, estimate water elevation:
   1. Store a list of elevations of boundary pixels for the feature, *boundary[f]*
   2. Initialize feature elevation *E[f] = 0*
   3. if (length(*boundary[f]*) > 0) then *E[f]* = *mean(boundary[f])*
6. For all water pixels *(i,j)*, calculate depth:
   1. if(*f[i,j]* > 0) then *d[i,j]* = max(0, *E[f[i,j]]* – *h[i,j]*)

The workflow outputs a GeoTIFF giving per-pixel water depth, with the same resolution and geolocation as the input classification map. The output for the scene in 5 (left – color, center – surface water extent) is shown in Figure 5 (right – water depth).

Several factors can impact the accuracy of this method. The classification of images itself is not

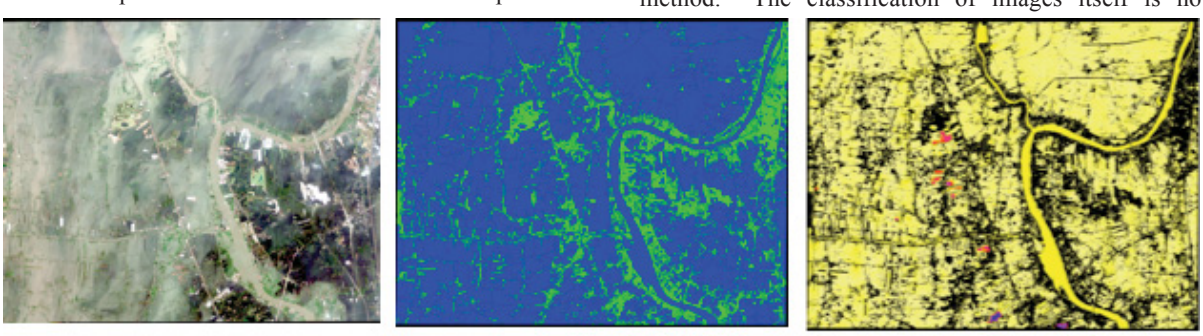

Figure 4: Browse image of GeoEye-1 scene of region north of Bangkok (image identifier: 2011111103572301603031609306 2-011111103572301603031609306_001) acquired November 11, 2011 (left);
surface water extent map calculated by thresholding G and NIR bands: blue = water, green = land (middle);
water depth map: pale yellow = 0 meters, blue = 13.7 meters (right). The water volume in the image is calculated as 465,000,000 m^3 at an average depth of 1.43 meters; however, this includes part of the Chao-Praya river.

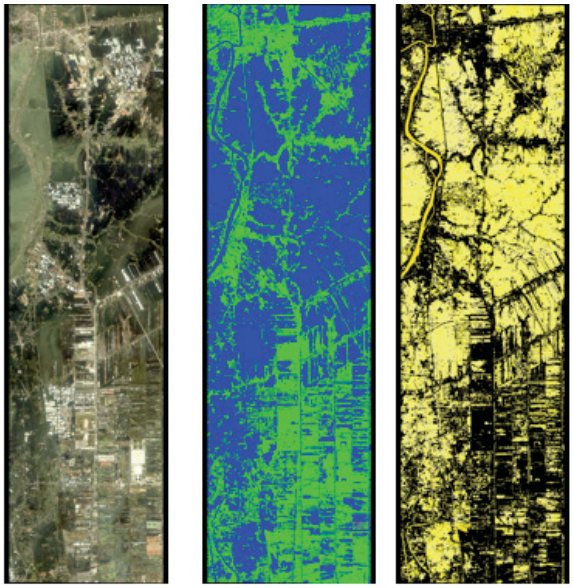

Figure 5: Browse image of IKONOS scene (image identifier: 2011110403545030000011624178200008284220 1THC) acquired over region north of Bangkok on November 4, 2011 (left); surface water extent map calculated by thresholding Green and NIR bands: blue = water, green = land (center); calculated water depth map: pale yellow = 0 meters, blue = 12.5 meters. The water volume in the image is estimated as 321,400,000 m^3 at an average depth of 1.30 meters.

perfect - not all land and water pixels can be reliably identified. Additionally, accurate geolocation in the classified output is essential to acquire elevation information from the DEM and derive accurate water depths. In the DEM itself, 1m jump in elevation represents a very large change compared to the roughly 2m average elevation for the city of Bangkok. The DEM data is also noisy; regions that would be expected to be flat in practice can be a mixture of pixels that differ by 1m in elevation. An elevation model with higher resolution would reduce noise and error in the water depth results.

It is also difficult to decide what to do with cloud or cloud shadow pixels, since it is unknown if these are flooded or not. It would be desirable to determine the status of these pixels based on the status of their neighbors. Currently, cloud pixels are treated as if they contain no data.

Finally, this method assumes that water level can be inferred by equating it with the elevation of surroundings, but this may not necessarily be true in urban environments.

The volumetric water estimation techniques have been applied to sensors beyond ALI: Worldview-2 (Figure 3), Geo-Eye-1 (Figure 4), Ikonos (Figure 5), Landsat,-7 and Radarsat-2 (Figures 6-8) (which has a shapefile product). Worldview-2, Ikonos, and Geo-Eye data enabled most precise volume estimation from its

Figure 6: Radarsat 2 polygonal surface water extent map. The shapefile extends all the way from Bangkok to northern Thailand. The image was taken November 11, 2011.

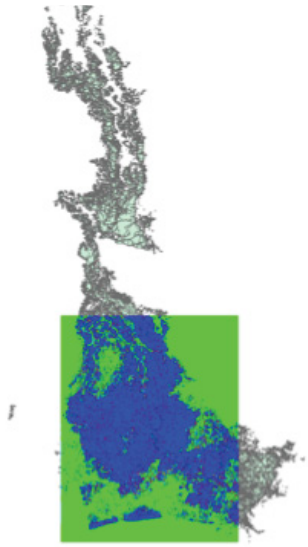

Figure 7: Rasterized water extent map: blue = flood water, green = land or permanent water. Generated within boundaries of Bangkok DEM, 25 meter resolution.

high spatial resolution (2m/pixel). Radarsat-2 highlights the all-weather strengths of radar. Figure 6 shows the original Radarsat-2 Shapefile product. In order to reuse our general workflow we rasterize this (Figure 7) then use our general workflow to estimate water volume (Figure 8). Landsat highlights the multi sensor applicability of the techniques. Figures 9-11 show Landsat-7 ETM-based tracking of flooding. We show gap-filled RGB, surface water extent, and water depth derived information, all derived from a Chao Praya scene from 17 Nov 2011.

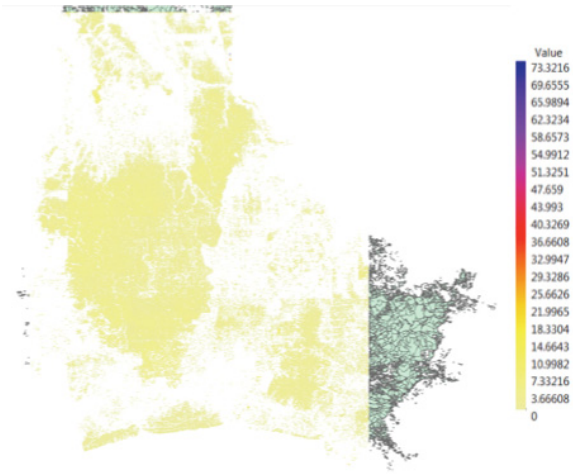

Figure 8: Radarsat-2 derived water volume. Zoomed in on water depth map, with scale at right. Maximum depth is given as 73 meters, but depths this extreme occur only in very small areas. Average depth of these pixels is 1.47 meters. The pale yellow pixels vary in depth up to about 3.5 meters. Total volume within this region estimated as 10,801,000,000 m^3.

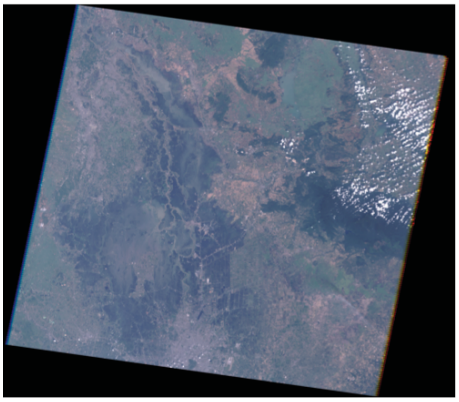

Figure 9: True color RGB Landsat7 ETM scene with gap filling from 17 Nov 2011. Bangkok (and flooded Don Muang airport) are visible on south side.

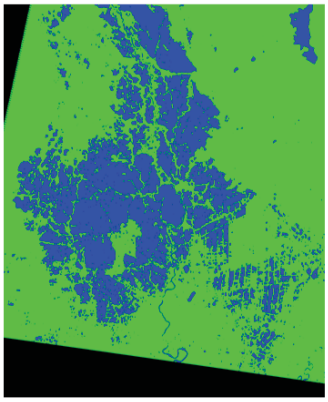

Figure 10: Surface water extent map 17 Nov 2011 classified using green / near infra-red ratio: blue = water, green = land, black = no data; only includes area within bounds of DEM.

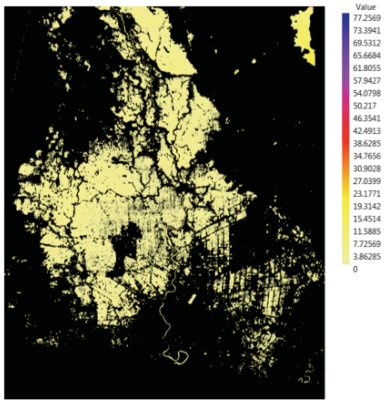

Figure 11: Water depth map derived from gap-filled imagery from 17 Nov 2011. Maximum water depth = 77.3 meters (tiny spot), average flooded pixel depth = 1.79m, total volume = 9,842,000,000 m^3. # of distinct water bodies: 1,761.

3.6 Implementation

All of the sensorweb software runs at servers located at the Jet Propulsion Laboratory, California Institute of Technology (JPL). MODIS data is downloaded from the LANCE-MODIS site to JPL where it is processed for flood detection. Relevant imaging requests are generated and transmitted electronically to the EO-1 tasking system resident at JPL [Chien et al. 2010]. Requests for other data are handled via a range of manual means including emails to crisis response points of contact. Response data is pulled automatically and semi-automatically from specific server sites and is then automatically processed into surface water extent and water depth products. These products are automatically electronically delivered to the Hydro Agro Informatics Institute (HAII) and Thaiflood.com to for access by and delivery to end users.

3.7 Experience using the Sensorweb in 2011-2012

We first deployed pieces of the sensorweb in the 2010 flooding season and added further capabilities in the 2011 flooding season. Working with authorities such as HAII, we identified 52 key monitoring sites in the Thailand region. From October 2011 to February 2012 (as this article goes to review) we operated the Thailand flood sensorweb.

During this period, we acquired almost 40 ALI scenes during the extended flooding. Of these approximately half of the scenes involved manual direction via user defined site priority. During this time Worldview-2, Geo-Eye1, Landsat-7, and Radarsat-2 acquired approximately 20 additional scenes that were used with the sensorweb to produce surface water extent and water volume products.

Using mostly automated workflows, the sensorweb enabled rapid targeting, processing, product generation, and electronic delivery of products to relevant organizations in Thailand via Thailflood.com and HAII. The only manual effort involved specific ALI image to digital elevation map registration and some tasking and data delivery for commercial sources. The end products were used for a range of purposes in flood response, tracking, and damage estimation.

4. DISCUSSION

We are continuing efforts to expand the sensorweb. We are working to integrate available in-situ data. Thailand's Hydro Agro Informatics Institute (HAII) processes data from over 200 in-situ stations including numerous rainfall, water level, and flow rate sensors (e.g. for the Mun river basin see http://www.thaiwater.net/DATA/REPORT/php/mun_scada/mun_scada.php). These in-situ sensors can provide valuable information on flooding by providing ground truth for rainfall, water depth, and flow rate/discharge. This information can also be used to direct other targetable sensors and to guide flood assessment.

HAII also operates river basin and sub-basin level hydrological models for all of the major rivers in Thailand. We are investigating mechanisms to automatically deliver the satellite data and in-situ sensor data to drive hydrological models to provide data for decision support in flood response. These hydrological models enable modeling and prediction of flooding caused by water flowing down river basins, often the most predictable of flood propagation.

The Thailand Flood Sensorweb to date has enabled rapid provision of high-resolution (meter scale) flood projects to end-users. By integrating and automating elements of detection, tasking, product generation, and product delivery it has enabled routine delivery of these products within days of acquisition.

Acknowledgements

Portions of this work were performed by the Jet Propulsion Laboratory, California Institute of Technology under contract with the National Aeronautics and Space Administration. Copyright 2012. All Rights reserved.

5. REFERENCES

1. MCOT – Ministry of Communication of Thailand, 19 November 2010, http://www.mcot.net/cfcustom/cache_page/131902.html
2. "FTI: Damage tally B50bn". Bangkok Post. http://www.bangkokpost.com/business/economics/204512/fti-damage-tally-b50bn. Retrieved 13 Nov 2010.
3. http://en.wikipedia.org/wiki/2010_Thai_floods, retrieved March 2011.
4. CNN. "Death toll in Thailand flooding rises to 206". CNN. http://edition.cnn.com/2010/WORLD/asiapcf/11/13/thailand.flooding.toll/. Retrieved 14 Nov 2010.
5. World Bank. http://www.worldbank.or.th/WBSITE/EXTERNAL/COUNTRIES/EASTASIAPACIFICEXT/THAILANDEXTN/0,,contentMDK:23067443~pagePK:141137~piPK:141127~theSitePK:333296,00.html Retrieved 18 February 2012
6. DFO – Dartmouth Flood Observatory, floodobservatory.colorado.edu, retrieved 20 February 2012.
7. G.R. Brakenridge and E. Anderson, "MODIS-Based Flood Detection, Mapping, and Measurement: The Potential for Operational Hydrological Applications," Transboundary Floods, Proc. NATO Advanced Research Workshop, Springer, 2005, pp. 1–12.
8. G.R. Brakenridge, S.V. Nghiem, E. Anderson, and S. Chien, "Space-based Measurement of River Runoff, EOS, Transactions AGU, vol. 86, No. 19, 10 May 2005, pp. 185-192.
9. GDACS, http://old.gdacs.org/flooddetection/, retrieved 26 June 2012.
10. OAS, http://oas.gsfc.nasa.gov/floodmap/ , retrieved 26 June 2012.
11. M. Carroll et al., "A New Global Raster Water Mask at 250 Meter Resolution," Int'l J. Digital Earth, vol. 2, no. 4, 2009.
12. M. L. Carroll, C. M. DiMiceli, J. R. G. Townshend, R. A. Sohlberg, P. Noojipady, P. (ongoing), MODIS Flood Maps, University of Maryland, College Park, Maryland.
13. G.R. Brakenridge, S.V. Nghiem, E. Anderson, and R. Mic, 2007, Orbital Microwave Measurement of River Discharge and Ice Status. Water Resources Research, v.43, W0405.
14. S. Chien, J. Doubleday, D. Mclaren, D. Tran, C. Khunboa, W. Leelapatra, V. Plergamon, V. Tanpipat, R. Chitradon, S. Boonya-aroonnet, P. Thanapakpawin, A. Meethome, C. Raghavendra, D. Mandl, "Combining Space-based and In-situ measurements to track flooding in Thailand," International Geoscience and Remote Sensing Symposium, Vancouver, BC, July (2011).
15. S. Chien, B. Cichy, A. G. Davies, D. Tran, G. Rabideau, R. Castano, R. Sherwood, D. Mandl, S. Frye, S. Schulman, J. Jones and S. Grosvenor (2005) An Autonomous Earth-Observing Sensorweb, IEEE Intelligent Systems, 20, no. 3, 16-24.
16. S. Chien, D. Tran, G. Rabideau, S. Schaffer, D. Mandl, S Frye, "Timeline-based Space Operations Scheduling with External Constraints, " International Conference on Automated Planning and Scheduling, Toronto, Canada, May 2010.
17. Ip, F., J. M. Dohm, V. R. Baker, T. Doggett, A. G. Davies, R. Castano, S. Chien, B. Cichy, R. Greeley, and R. Sherwood (2005) Development and Testing of the Autonomous Spacecraft Experiment (ASE) floodwater classifiers: Real-time Smart Reconnaissance of Transient Flooding. Remote Sensing of Environment, V. 101 #4, pp. 463-481.
18. Schölkopf, B., & Smola, A. J. (2002). Learning with kernels. Cambridge, MA: MIT Press.
19. D. Mclaren, J. Doubleday, S. Chien, Using WorldView-2 imagery to track flooding in Thailand in a multi-asset sensorweb, SPIE Defense, Security + Sensing 2012, Baltimore, MD, April 2012.
20. Pixellearn, NASA Tech Briefs, November 2006.